Received: 16 October 2022 | Accepted: 3 November 2022

DOI: 10.1002/pamm.202200323

Methods of Model Order Reduction for Coupled Systems Applied to a Brake Disc-Wheel Composite

Fabian Matter[1], **Igor Iroz**[2], and **Peter Eberhard**[1,*]

[1] University of Stuttgart, Institute of Engineering and Computational Mechanics, Pfaffenwaldring 9, 70569 Stuttgart, Germany

[2] Dr. Ing. h.c. F. Porsche Aktiengesellschaft, Porschestraße 911, 71287 Weissach, Germany

In this contribution, investigations on model order reduction for coupled systems composed from components of a passenger car are shown. In today's development processes, the simulation of mechanical components is indispensable and large Finite Element models are often used for this purpose. For the calculation of time-domain or frequency-domain analyses, for example, a lot of computing power is required. However, with the application of model order reduction methods, this effort can be reduced, but this results in a trade-off between the reduction error and the computational time. Since the computation of reduction bases for complete systems can be computationally expensive, it is of interest to be able to reduce components individually and then assemble them into a reduced overall model. This can result in both, a saving of computational effort when creating the bases, as well as a saving of the required memory space. Furthermore, there are many possible combinations of components in the modular systems of today's automotive industry, which emphasizes the model order reduction by parts and not by assemblies. In this work, methods of model order reduction for coupled systems are presented and will be tested on components in the chassis of a sports car. Therefore, an assembly consisting of a brake disc and wheel rim together with the wheel hub are investigated. For this purpose, the eigenmodes and transfer functions of the overall model, the reduced overall model and the assembly built from individual reduced bodies are compared.

1 Introduction

The phenomenon of brake squeal has been subject to research and development for several decades and is extremely complex, so it continues to be studied. An overview of brake squeal and the methods used to investigate and predict it can be found in [1]. Today, more and more expensive bench testing is being replaced by computer simulation to identify system characteristics during the development. In the field of brake squeal analysis, both frequency domain and time domain analyses need to be used. In the frequency domain analysis, the complex eigenvalue analysis has been established. In the time domain, the simulation as a flexible multibody system has proven useful, see [2]. However, regardless of the type of simulation, model order reduction (MOR) has become increasingly important, because the description of brakes as Finite Element models results in very detailed and large models. With the help of MOR, large models can be reduced to smaller models, which can still contain enough information to describe the system behavior sufficiently well. However, the quality is strongly dependent on the used method and the reduction size. An overview of linear MOR methods in the field of elastic bodies can be found in [3] and [4]. To meet the trend of modular designed technical products and to exploit these properties, special reduction methods for coupled structures have been designed, see [5]. These methods are also particularly well suited to meet the configuration variety in the automotive industry and to create efficient simulation models. In this work, new methods of MOR such as the CMS-GRAM method, which was developed specifically for coupled structures, will be investigated using an assembly of a brake rotor, a rim and a wheel hub. In the first section, MOR for coupled systems is discussed. In the following section, the investigated model is described in more detail. In the last section, corresponding simulation results are presented.

2 Model order reduction for substructured systems

First, the fundamental equations for the description of elastic bodies are explained and subsequently the method of model order reduction by projection is introduced. Based on this, the equations for the coupling of reduced bodies are introduced. In this contribution, we focus on the coupling with algebraic bindings.

By describing an elastic body with the linear Finite Element method, we obtain the discretized equation of motion for one body

$$\boldsymbol{M}\ddot{\boldsymbol{q}}(t) + \boldsymbol{D}\dot{\boldsymbol{q}}(t) + \boldsymbol{K}\boldsymbol{q}(t) = \boldsymbol{f}(t), \tag{1}$$

with the mass matrix $\boldsymbol{M} \in \mathbb{R}^{N\times N}$, the damping matrix $\boldsymbol{D} \in \mathbb{R}^{N\times N}$, the stiffness matrix $\boldsymbol{K} \in \mathbb{R}^{N\times N}$ and the force vector $\boldsymbol{f} \in \mathbb{R}^{N}$. Using model order reduction, a structurally identical equation of motion is sought which has a significantly smaller

* Corresponding author: e-mail peter.eberhard@itm.uni-stuttgart.de, phone +49 711 685 -66388, fax +49 711 685 -66400

dimension $n \lll N$. This is achieved by a Galerkin projection with a projection matrix $\boldsymbol{V}$. The vector of the generalized reduced coordinates is then defined as

$$\boldsymbol{q}(t) \approx \boldsymbol{V}\tilde{\boldsymbol{q}}(t). \tag{2}$$

Substituting the relation for the generalized, reduced coordinates into Equation (1) and multiplying the equation of motion by $\boldsymbol{V}^\intercal$ from left due to the Petrov-Galerkin projection, yields to

$$\boldsymbol{V}^\intercal\boldsymbol{M}\boldsymbol{V}\ddot{\boldsymbol{q}}(t) + \boldsymbol{V}^\intercal\boldsymbol{D}\boldsymbol{V}\dot{\boldsymbol{q}}(t) + \boldsymbol{V}^\intercal\boldsymbol{K}\boldsymbol{V}\boldsymbol{q}(t) = \boldsymbol{V}^\intercal\boldsymbol{f}(t). \tag{3}$$

This corresponds to the equation of motion of the reduced model of one elastic body

$$\tilde{\boldsymbol{M}}\ddot{\tilde{\boldsymbol{q}}}(t) + \tilde{\boldsymbol{D}}\dot{\tilde{\boldsymbol{q}}}(t) + \tilde{\boldsymbol{K}}\tilde{\boldsymbol{q}}(t) = \tilde{\boldsymbol{f}}(t). \tag{4}$$

2.1 Coupling of reduced systems with algebraic bindings

Since the focus of this contribution is on the application of reduction methods for substructured systems, the underlying equations for coupling reduced systems based on algebraic bindings are explained. For a detailed description, the reader is referred to [5]. There, both the coupling methods and the reduction methods are described in detail.

Each single reduced subsystem k with dimension n_k is subjected to constraint forces due to the couplings and thus the equation of motion of a single reduced subsystem is given by

$$\tilde{\boldsymbol{M}}_k\ddot{\tilde{\boldsymbol{q}}}_k(t) + \tilde{\boldsymbol{D}}_k\dot{\tilde{\boldsymbol{q}}}_k(t) + \tilde{\boldsymbol{K}}_k\tilde{\boldsymbol{q}}_k(t) = \tilde{\boldsymbol{f}}_k(t) + \tilde{\mathfrak{f}}_k(t) \tag{5a}$$

$$\text{with} \qquad \tilde{\boldsymbol{M}}_k = \boldsymbol{V}_k^\intercal\boldsymbol{M}_k\boldsymbol{V}_k, \qquad \tilde{\boldsymbol{D}}_k = \boldsymbol{V}_k^\intercal\boldsymbol{D}_k\boldsymbol{V}_k, \qquad \tilde{\boldsymbol{K}}_k = \boldsymbol{V}_k^\intercal\boldsymbol{K}_k\boldsymbol{V}_k, \tag{5b}$$

$$\tilde{\boldsymbol{f}}_k(t) = \boldsymbol{V}_k^\intercal\boldsymbol{f}_k(t), \qquad \tilde{\mathfrak{f}}_k(t) = \boldsymbol{V}_k^\intercal\mathfrak{f}_k(t). \tag{5c}$$

Hereby $\mathfrak{f}_k(t) \in \mathbb{R}^{N_k}$ is the vector of the constraint forces of the unreduced subsystem k. It results for the coupled system of reduced systems the dimension $n = \sum_{k=1}^{K} n_k$. Therefore, the equation of motion has the form

$$\tilde{\boldsymbol{M}}\ddot{\tilde{\boldsymbol{q}}}(t) + \tilde{\boldsymbol{D}}\dot{\tilde{\boldsymbol{q}}}(t) + \tilde{\boldsymbol{K}}\tilde{\boldsymbol{q}}(t) = \tilde{\boldsymbol{f}}(t) + \tilde{\mathfrak{f}}(t) \tag{6a}$$

$$\text{with} \qquad \tilde{\boldsymbol{M}} = \operatorname{diag}(\tilde{\boldsymbol{M}}_1, ..., \tilde{\boldsymbol{M}}_K), \tag{6b}$$

$$\tilde{\boldsymbol{D}} = \operatorname{diag}(\tilde{\boldsymbol{D}}_1, ..., \tilde{\boldsymbol{D}}_K), \tag{6c}$$

$$\tilde{\boldsymbol{K}} = \operatorname{diag}(\tilde{\boldsymbol{K}}_1, ..., \tilde{\boldsymbol{K}}_K), \tag{6d}$$

$$\tilde{\boldsymbol{q}}(t) = \begin{bmatrix} \tilde{\boldsymbol{q}}_1(t) \\ \vdots \\ \tilde{\boldsymbol{q}}_K(t) \end{bmatrix}, \qquad \tilde{\boldsymbol{f}}(t) = \begin{bmatrix} \tilde{\boldsymbol{f}}_1(t) \\ \vdots \\ \tilde{\boldsymbol{f}}_K(t) \end{bmatrix}, \qquad \tilde{\mathfrak{f}}(t) = \begin{bmatrix} \tilde{\mathfrak{f}}_1(t) \\ \vdots \\ \tilde{\mathfrak{f}}_K(t) \end{bmatrix}. \tag{6e}$$

Since in our case the constraint forces are not of special interest, it is useful to represent the system in minimal coordinates $\tilde{\boldsymbol{q}}_m$. The minimum coordinates of the system represent the feasible deformations under compliance with $\mathfrak{p}$ constraints. The compatibility condition, which states that the respective positions at the coupling points coincide at all times, is expressed by the algebraic binding equations,using the generalized reduced coordinates $\tilde{\boldsymbol{q}}(t)$

$$\tilde{\boldsymbol{J}}\tilde{\boldsymbol{q}}(t) = \boldsymbol{0} \qquad \text{with} \qquad \tilde{\boldsymbol{J}} = \boldsymbol{J}\boldsymbol{V} \qquad \boldsymbol{V} = \operatorname{diag}(\boldsymbol{V}_1, ..., \boldsymbol{V}_K). \tag{7}$$

Here $\tilde{\boldsymbol{J}} \in \mathbb{R}^{\mathfrak{p}\times n}$ is the Jacobian matrix of the bindings and must have full row rank to satisfy the constraints with the set of reduced coordinates. To find a appropriate set of minimal coordinates $\tilde{\boldsymbol{q}}_m$, which is valid for

$$\tilde{\boldsymbol{q}}(t) = \tilde{\boldsymbol{L}}\tilde{\boldsymbol{q}}_m(t), \qquad \tilde{\boldsymbol{q}} : \tilde{\boldsymbol{J}}\tilde{\boldsymbol{q}}(t) = \tilde{\boldsymbol{J}}\tilde{\boldsymbol{L}}\tilde{\boldsymbol{q}}_m(t) = \boldsymbol{0} \quad \forall\tilde{\boldsymbol{q}}_m(t), \qquad \tilde{\boldsymbol{q}}_m \in \mathbb{R}^{n-\mathfrak{p}}, \tag{8}$$

a matrix $\tilde{\boldsymbol{L}} \in \mathbb{R}^{n\times n-\mathfrak{p}}$ is needed. This matrix has typically the form of a Boolean matrix and can be determined with a QR-decomposition. With this matrix, the equation of motion in generalized, reduced coordinates in Equation (6a) can be transformed to minimal form with $n - \mathfrak{p}$ degrees of freedom (DOFs) as

$$\tilde{\boldsymbol{M}}_m\ddot{\tilde{\boldsymbol{q}}}_m(t) + \tilde{\boldsymbol{D}}_m\dot{\tilde{\boldsymbol{q}}}_m(t) + \tilde{\boldsymbol{K}}_m\tilde{\boldsymbol{q}}_m(t) = \tilde{\boldsymbol{f}}_m(t). \tag{9}$$

2.2 CMS-GRAM

The new method CMS-Gram, which was introduced for the first time in [5], is a new reduction method for substructured systems. It connects the advantages of interpolation-based methods and balanced truncation. Thus, the size of the reduced substructure is not necessarily a multiple of the expansion points of the moment matching methods, whose choice is a nontrivial problem [4]. In this method, similar to the Guyan condensation [6], the degrees of freedom are divided and sorted into internal DOFs (subscript i) and boundary DOFs (subscript b). The input and output matrices and the matrix of constraints are also split accordingly. This results in the following equation for a single substructure

$$\begin{bmatrix} \boldsymbol{M}_{\mathrm{bb}} & \boldsymbol{M}_{\mathrm{bi}} \\ \boldsymbol{M}_{\mathrm{ib}} & \boldsymbol{M}_{\mathrm{ii}} \end{bmatrix} \begin{bmatrix} \ddot{\boldsymbol{q}}_b \\ \ddot{\boldsymbol{q}}_i \end{bmatrix} + \begin{bmatrix} \boldsymbol{K}_{\mathrm{bb}} & \boldsymbol{K}_{\mathrm{bi}} \\ \boldsymbol{K}_{\mathrm{ib}} & \boldsymbol{K}_{\mathrm{ii}} \end{bmatrix} \begin{bmatrix} \dot{\boldsymbol{q}}_b \\ \dot{\boldsymbol{q}}_i \end{bmatrix} = \begin{bmatrix} \boldsymbol{J}_{\mathrm{b}}^{\intercal} & \boldsymbol{B}_{\mathrm{b}} \\ \boldsymbol{0} & \boldsymbol{B}_{\mathrm{i}} \end{bmatrix} \begin{bmatrix} \mathfrak{u} \\ \boldsymbol{u} \end{bmatrix}, \tag{10a}$$

$$\boldsymbol{y} = \begin{bmatrix} \boldsymbol{C}_b & \boldsymbol{C}_b \end{bmatrix} \begin{bmatrix} \boldsymbol{C}_b \\ \boldsymbol{C}_i \end{bmatrix}. \tag{10b}$$

Then a coordinate transformation is performed with the transformed internal coordinates $\hat{\boldsymbol{q}}_i$ and with the relation

$$\boldsymbol{V}_{\mathrm{T}} = \begin{bmatrix} \boldsymbol{I} & \boldsymbol{0} \\ \boldsymbol{\Psi}_{\mathrm{i}} & \boldsymbol{I} \end{bmatrix} \in \mathbb{R}^{N \times N}, \qquad \begin{bmatrix} \boldsymbol{q}_{\mathrm{b}} \\ \boldsymbol{q}_{\mathrm{i}} \end{bmatrix} = \boldsymbol{V}_{\mathrm{T}} \begin{bmatrix} \boldsymbol{q}_{\mathrm{b}} \\ \hat{\boldsymbol{q}}_{\mathrm{i}} \end{bmatrix}, \tag{11}$$

where $\boldsymbol{\Psi_{\mathrm{i}}}$ is determined by a static condensation. If the transformation is applied to Equation (10) it follows

$$\begin{bmatrix} \hat{\boldsymbol{M}}_{\mathrm{bb}} & \boldsymbol{M}_{\mathrm{bi}} + \boldsymbol{\Psi}_{\mathrm{i}}^{\intercal} \boldsymbol{M}_{\mathrm{ii}} \\ \hat{\boldsymbol{M}}_{\mathrm{ib}} + \boldsymbol{M}_{\mathrm{ii}} \boldsymbol{\Psi}_{\mathrm{i}} & \boldsymbol{M}_{\mathrm{ii}} \end{bmatrix} \begin{bmatrix} \ddot{\boldsymbol{q}}_{\mathrm{b}} \\ \ddot{\hat{\boldsymbol{q}}}_{\mathrm{i}} \end{bmatrix} + \begin{bmatrix} \hat{\boldsymbol{K}}_{\mathrm{bb}} & \boldsymbol{K}_{\mathrm{bi}} + \boldsymbol{\Psi}_{\mathrm{i}}^{\intercal} \boldsymbol{K}_{\mathrm{ii}} \\ \hat{\boldsymbol{K}}_{\mathrm{ib}} + \boldsymbol{K}_{\mathrm{ii}} \boldsymbol{\Psi}_{\mathrm{i}} & \boldsymbol{K}_{\mathrm{ii}} \end{bmatrix} \begin{bmatrix} \boldsymbol{q}_{\mathrm{b}} \\ \hat{\boldsymbol{q}}_{\mathrm{i}} \end{bmatrix} = \begin{bmatrix} \boldsymbol{J}_{\mathrm{b}}^{\intercal} & \hat{\boldsymbol{B}}_{\mathrm{b}} \\ \boldsymbol{0} & \boldsymbol{B}_{\mathrm{i}} \end{bmatrix} \begin{bmatrix} \mathfrak{u} \\ \boldsymbol{u} \end{bmatrix}, \tag{12a}$$

$$\boldsymbol{y} = \begin{bmatrix} \hat{\boldsymbol{C}}_{\mathrm{b}} & \boldsymbol{C}_{\mathrm{i}} \end{bmatrix} \begin{bmatrix} \boldsymbol{q_b} \\ \hat{\boldsymbol{q}}_i \end{bmatrix} \tag{12b}$$

with

$$\hat{\boldsymbol{M}}_{\mathrm{bb}} = \boldsymbol{M}_{\mathrm{bb}} + \boldsymbol{M}_{\mathrm{bi}} \boldsymbol{\Psi}_{\mathrm{i}} + \boldsymbol{\Psi}_{\mathrm{i}}^{\intercal} \boldsymbol{M}_{\mathrm{ib}} + \boldsymbol{\Psi}_{\mathrm{i}}^{\intercal} \boldsymbol{M}_{\mathrm{ii}} \boldsymbol{\Psi}_{\mathrm{i}}, \tag{13a}$$

$$\hat{\boldsymbol{K}}_{\mathrm{bb}} = \boldsymbol{K}_{\mathrm{bb}} + \boldsymbol{K}_{\mathrm{bi}} \boldsymbol{\Psi}_{\mathrm{i}} + \boldsymbol{\Psi}_{\mathrm{i}}^{\intercal} \boldsymbol{K}_{\mathrm{ib}} + \boldsymbol{\Psi}_{\mathrm{i}}^{\intercal} \boldsymbol{K}_{\mathrm{ii}} \boldsymbol{\Psi}_{\mathrm{i}}, \tag{13b}$$

$$\hat{\boldsymbol{B}}_{\mathrm{b}} = \boldsymbol{B}_{\mathrm{b}} + \boldsymbol{\Psi}_{\mathrm{i}}^{\intercal} \boldsymbol{B}_{\mathrm{i}}, \tag{13c}$$

$$\hat{\boldsymbol{C}}_{\mathrm{b}} = \boldsymbol{C}_{\mathrm{b}} + \boldsymbol{\Psi}_{\mathrm{i}}^{\intercal} \boldsymbol{C}_{\mathrm{i}}. \tag{13d}$$

A linear reduction method, the balanced truncation, see [3], is now applied to the internal dynamics, which are described by

$$\boldsymbol{M}_{\mathrm{ii}} \ddot{\hat{\boldsymbol{q}}} + \boldsymbol{K}_{\mathrm{ii}} \dot{\hat{\boldsymbol{q}}} = \begin{bmatrix} \boldsymbol{B}_{\mathrm{i}} & -(\boldsymbol{M}_{\mathrm{ib}} + \boldsymbol{M}_{\mathrm{ii}} \Psi_{\mathrm{i}}) \end{bmatrix} \begin{bmatrix} \boldsymbol{u} \\ \ddot{\boldsymbol{q}}_{\mathrm{b}} \end{bmatrix} \tag{14}$$

and then the projection matrix $\boldsymbol{V}_{\mathrm{i}}$ is determined. In combination with the static modes the projection matrix

$$\boldsymbol{V}_{\mathbf{CMSG}} = \begin{bmatrix} \boldsymbol{I} & \boldsymbol{0} \\ \boldsymbol{\Psi_i} & \boldsymbol{V}_i \end{bmatrix} \tag{15}$$

for one substructure is obtained.

3 Numerical Model

In the following we use a Finite Element model of a brake rotor, a rim and a wheel hub. The assembly is shown in Figure 1a. For the parts different material properties are used, which can be seen in Table 1. Furthermore, the assembly, which consists of the three parts, has about $1.21 \cdot 10^6$ DOFs. Normally, the three parts are screwed together with five wheel bolts and the wheel bolts are screwed into the threads in the wheel hub, but in our numerical model the screws are not modeled as a part. Instead of this we use algebraic bindings for assembling the parts. For this purpose, for each part five guiding nodes are defined, respectively one for each bore. The guiding nodes are shown in Figure 1b. The guiding node of one part is located in the center of the bore. Furthermore, one can see the connections from the guiding node to the dependent nodes as a purple line. The guiding node has the property that it leads the movement of the dependent nodes. To assemble the parts, algebraic bindings are defined between the guiding nodes of each bore. Consequently, we have five bindings here, which connect a part with the adjacent part. Furthermore, it is mentioned, that in this contribution a free fixation of the assembly is used for the numerical investigations. This has the advantage that the results can be easily compared with those of Laser Doppler Vibrometry.

Table 1: Material and mesh properties of the investigated model

	rim	brake rotor	wheel hub
density	aluminum: 2700 kg/m3	aluminum: 2700 $\mathrm{kg/m^3}$ steel: 7850 $\mathrm{kg/m^3}$ cast iron: 7250 $\mathrm{kg/m^3}$	steel: 7850 $\mathrm{kg/m^3}$
Young modulus	aluminum: 70000 MPa	aluminum: 70000 MPa steel: 210000 MPa cast iron: 86000 MPa	steel: 210000 Mpa

(a) Iso-view of the discretized assembly, consisting of the rim (green), a brake rotor (mint) and a wheel hub (yellow).

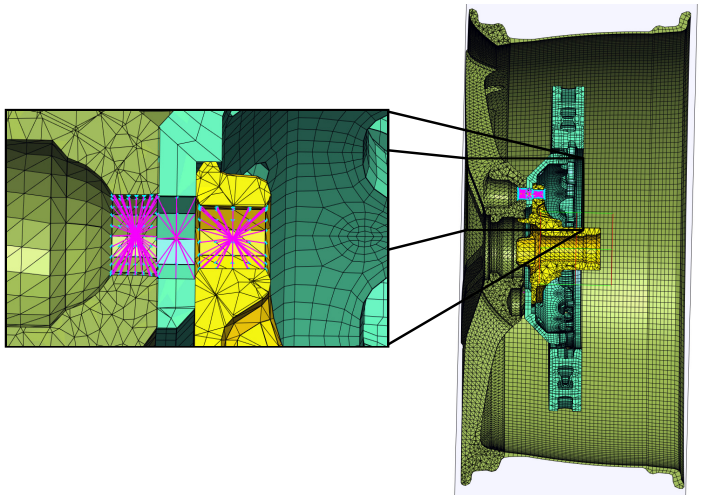

(b) Sectional view of the assembly with enlarged section on the multi point constraints, which consist of the guiding node in the center and the dependent nodes located at the outside of the bore.

4 Simulation Results

In the following section, simulation results are presented and discussed. For the comparison of the methods, two different tests were performed. First, the modal assurance criterion (MAC) was calculated, which is very suitable for comparing eigenmodes with each other, see [7]. Also, the transfer functions of the full and the reduced models were calculated. In order to be able to compare the transfer functions, it is useful to consider the Frobenius norm of the transfer functions, see [8]. Thus, the Frobenius norm of the transfer functions and its error are calculated in the following.

In Figure 2 the transfer functions of the full model and different reduced overall models are shown. As a typical case we have chosen the modal truncation with the first 1000 eigenmodes. In comparison to the moment matching method the number of modes is higher in order to cover the whole frequency range. In the low frequency range until approximately 300 Hz a divergence between the modal reduced model and the full model is visible, but at higher frequencies the divergence is getting lower. In comparison to the modal reduced model also a moment matching method witch Krylov subspaces is used. In Figure 2 two graphs are shown. One reduced system is of the size 50 and the other one of the size 200. It is cognizable that with only 200 modes the transmission behaviour of the full system is matched very well. The corresponding error of the transfer function is shown in Figure 4. In Figure 2 the Kry 200 graph lies exactly on the black one for the full model. Now, Figure 3 additionally shows the transfer functions of the CMS Gram reduced models in rose for Gram 200, and purple for Gram 400. In this case it should be mentioned that, for the reduction 200 and respectively 400 modes for the reduction of each part is used. Thus, the total system size of 600 and 1200 modes respectively, is comparable to the used modal truncation. It is noticeable that the transfer behavior is not approximated as well as with the methods already shown. It is also understandable that the result quality tends to be worse with the CMS Gram method, since the errors caused by the individual reductions of the components and the subsequent assembly also add up. Generally speaking the amplification is mapped higher in the whole frequency range. However, the peaks at the natural frequencies are still represented very well. As already mentioned, the eigenmodes were compared in addition to the transmission behavior. For this purpose, the MAC of the first 20 eigenmodes was calculated. The results are shown in Figure 5a and Figure 5b. In both figures only one main diagonal is visible, which means that with both methods the eigenmodes are approximated very well.

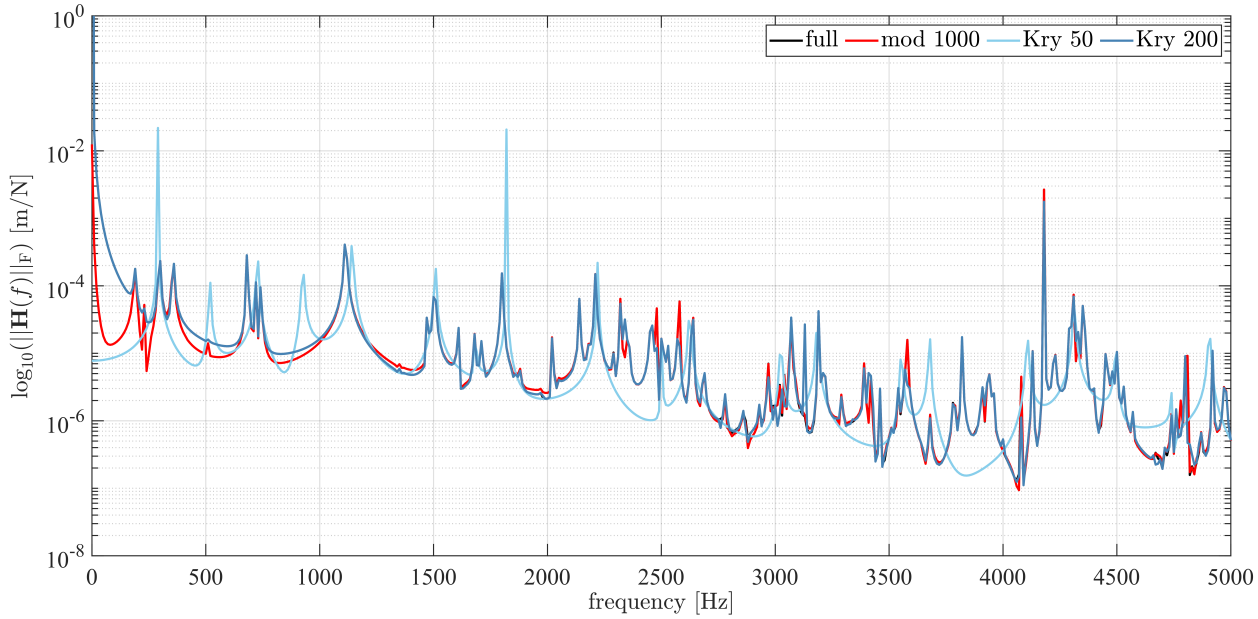

Fig. 2: Transfer functions of the full model and different reduced overall models

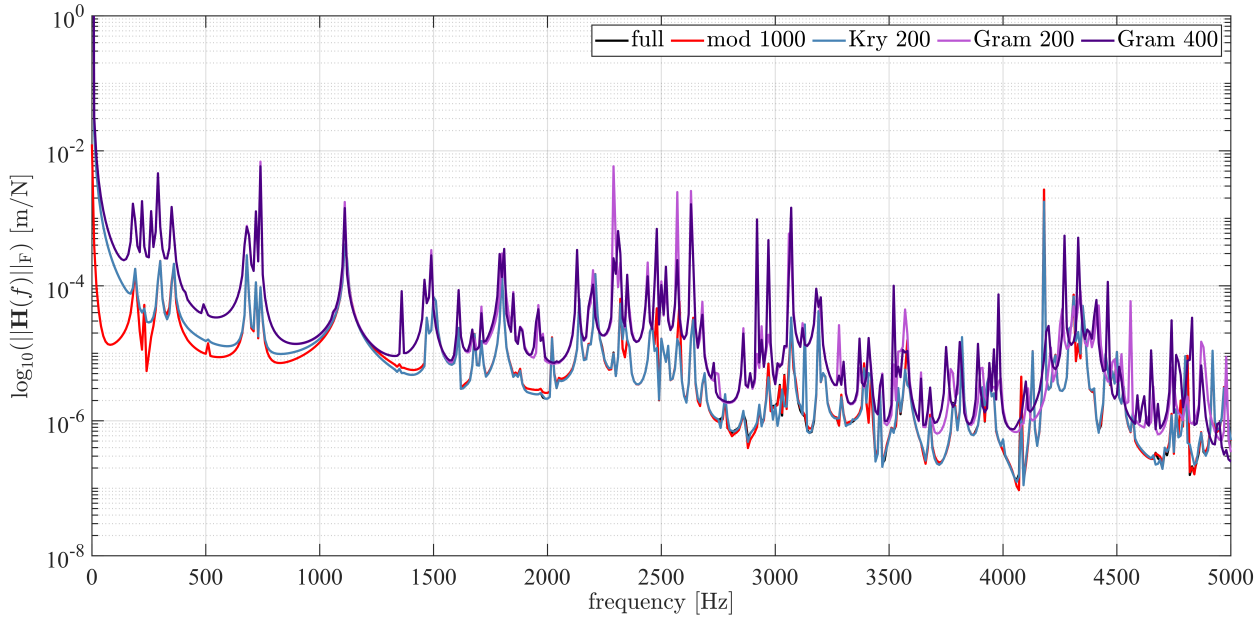

Fig. 3: Comparison of the transfer function of different reduced models

5 Conclusion

In this work, different reduction methods were applied on a coupled system. The system consists of three components, which are assembled with algebraic bindings. This kind of coupling allows to model a rigid bond of the components. In addition to the classical established reduction methods applied to the assembly, a new reduction method for substructured systems, presented in [5], was also applied. This method allows the parts to be reduced before assembly and so to work with reduced models during the assembly generation which in turn saves computation time and memory. To evaluate the model quality, both the transmission behavior and the MAC were calculated. It could be shown that a very good approximation of the eigenvectors can be represented with the classical reduction methods for the overall system as well as with the CMS-Gram method. In the transmission behavior, however, smaller errors were achieved with the modal truncation and the moment matching method. Beside the CMS-Gram method there are more reduction methods for substructured systems, e.g. the Craig-Bampton method, see [9], or the block-Krylov method. Thus, a comparison of these methods is suggested.

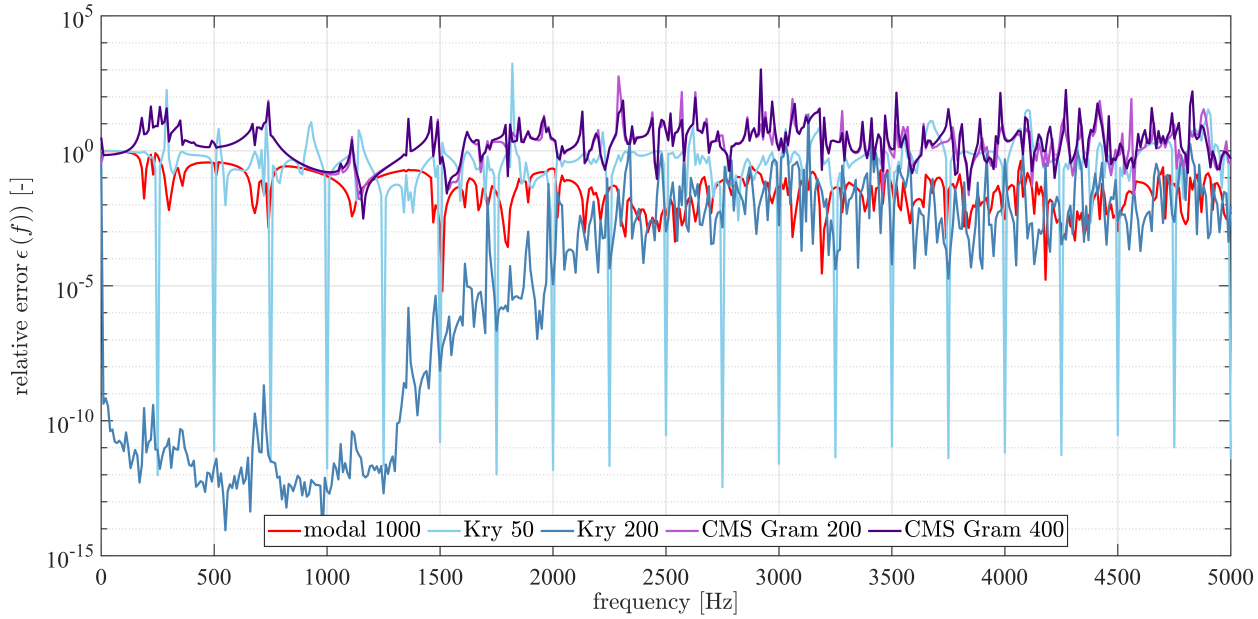

Fig. 4: Error of the transfer functions of different reduced models

(a) MAC values of the Krylov reduced system

(b) MAC values of the CMS-Gram reduced system

Fig. 5: MAC values of the first 20 eigenmodes of different reduction methods

Acknowledgements Open access funding enabled and organized by Projekt DEAL.

References

[1] N. Kinkaid, O. O'Reilly, and P. Papadopoulos, Automotive disc brake squeal, Journal of Sound and Vibration **267**(1), 105 – 166 (2003).
[2] I. Iroz, Simulation of Friction-Induced Vibrations in Automotive Brake Systems, Doctoral thesis, Schriften aus dem Institut für Technische und Numerische Mechanik der Universität Stuttgart, Vol. 56 (Shaker Verlag, Aachen, 2018).
[3] M. Lehner, Modellreduktion in elastischen Mehrkörpersystemen, Doctoral thesis, Schriften aus dem Institut für Technische und Numerische Mechanik der Universität Stuttgart, Vol. 10 (Shaker Verlag, Aachen, 2007).
[4] J. Fehr, Automated and Error-Controlled Model Reduction in Elastic Multibody Systems, Doctoral thesis, Schriften aus dem Institut für Technische und Numerische Mechanik der Universität Stuttgart, Vol. 21 (Shaker Verlag, Aachen, 2011).
[5] P. Holzwarth, Modellordnungsreduktion für substrukturierte mechanische Systeme, Doctoral thesis, Schriften aus dem Institut für Technische und Numerische Mechanik der Universität Stuttgart, Vol. 51 (Shaker Verlag, Aachen, 2017).
[6] R. J. Guyan, Reduction of stiffness and mass matrices, AIAA Journal **3**(2), 380 (1965).
[7] R. J. Allemang The modal assurance criterion – twenty years of use and abuse, Journal of Sound and Vibration **37**(8), 14–21 (2003).
[8] A. Antoulas, Approximation of Large-Scale Dynamical Systems (SIAM, Philadelphia, 2005).
[9] R. Craig, Coupling of substructures for dynamic analyses: an overview, in: Proceedings of the AIAA Dynamics Specialists Conference, (Atlanta, 2000).

